J Math Chem (2011) 49:475–488
DOI 10.1007/s10910-010-9753-8

ORIGINAL PAPER

Modelling the joining of nanocones and nanotubes

Duangkamon Baowan · Barry J. Cox · James M. Hill

Received: 12 January 2010 / Accepted: 4 October 2010 / Published online: 16 October 2010

Abstract Carbon nanocones have been proposed as probes for scanning tunnelling microscopes, but there is currently no precise procedure to design such a nano-device. The successful design of many novel nano-electronic devices may require a thorough understanding of the geometric joining issues of certain nanostructures. In this paper, we propose a calculus of variations model of the composite nanostructure obtained by joining a carbon nanocone and a carbon nanotube. We propose a continuous approximation to the discrete composite structure and we assume rotational symmetry of the proposed nanostructure, so that the three dimensional problem can be reduced to a problem in two dimensions. In making these assumptions, we recognise that the existence of pentagons in the cone may result in some minor undulations of the proposed axially symmetric structure. However, our purpose is to formulate the basic underlying structure from which any such small perturbations may be viewed as departures from an ideal model. We examine two models depending upon the curvature of the join profile which can be either positive or both positive and negative. There is at present no experimental or simulation data for comparison with the theoretical connecting structures predicted by this study, which in itself is some justification for the proposed simple model presented here.

Keywords Carbon nanocones · Carbon nanotubes · Calculus of variations

D. Baowan (✉)
Department of Mathematics, Faculty of Science, Mahidol University, Bangkok 10400, Thailand
e-mail: scdbw@mahidol.ac.th

D. Baowan
Centre of Excellence in Mathematics, CHE, Si Ayutthaya Rd., Bangkok 10400, Thailand

B. J. Cox · J. M. Hill
Nanomechanics Group, School of Mathematical Sciences, The University of Adelaide, Adelaide, SA 5005, Australia

1 Introduction

Carbon nanostructures are believed to be unique materials which may be used as components to create many novel nano-devices. Most of the current research effort centres on the use of carbon nanotubes and C_{60}-fullerenes. To date there has been very little work undertaken on carbon nanocones. One reason for this is that only a small amount of carbon nanocones are produced during synthesis [1]. Carbon nanocones were first discovered by Ge and Sattler [2] and subsequently synthesised by Krishnan et al. [3]. They are formed from a graphene sheet with the disclination number of pentagons $N_p = 1, 2, 3, 4$ or 5, so that there are five possible non-trivial ways to create a carbon nanocone. As a consequence of Euler's theorem, the cap of a carbon nanotube consists of six pentagons, and we note that for $N_p = 6$ we obtain a capped carbon nanotube, and $N_p = 0$ corresponds to a graphene sheet. For a regular polyhedron comprising only hexagons and pentagons, Euler's theorem (Faces plus Vertices equals Edges plus 2) gives immediately $N_p = 6$ for any closed cap, so that for example any fullerene C_m contains precisely 12 pentagons. Assuming that the cone vertex angle is given by γ, then the two trivial and five non-trivial values of γ are shown in Table 1.

Most research on carbon nanocones deals with their electronic structure [4,5], and it is generally believed that the different number of pentagons in carbon nanocones is the key to the puzzle of nucleation in atomic construction. Pincak and Osipov [5] find that the electron states depend on the position of the pentagons. Moreover, because of their local density properties Charlier and Rignanese [4] have proposed carbon nanocones as the ideal candidates for the probes of scanning tunnelling microscopes. Quite recently Yeh et al. [6] and Zhang et al. [7] grow and investigate the field emission properties of one-dimensional composite carbon structures, comprising single-walled carbon nanotubes with nanocone tips.

In this paper, we utilise classical applied mathematical modelling and the calculus of variations, to determine the join between a carbon nanocone and a carbon nanotube, so that the combined structure might be used as a probe for scanning tunnelling microscopy (see Fig. 1). Fundamental to the model presented here, is the assumption of axial symmetry. We recognise that in reality the inclusion of pentagons in the cone may well violate this assumption, and the approach adopted here is to accommodate the major features to encapsulate the dominant physical effects. The existence of pentagons might be expected to cause small perturbations from an otherwise axially symmetric system. In the first instance, our purpose is to formulate the underlying axially symmetric model so that we may envisage a real physical system in terms of the departures from an ideal model. Also we comment that here we propose a continuous approximation to an essentially discrete composite structure. In proposing such an approach we have in mind the determination of a simple useful model, which might overall provide a reasonably accurate approximation to an otherwise extremely

Table 1 Relation of number of pentagons N_p and open angle γ for carbon nanocones

N_p	0	1	2	3	4	5	6
γ (°)	180	112.90	83.60	60.00	38.90	19.2	0

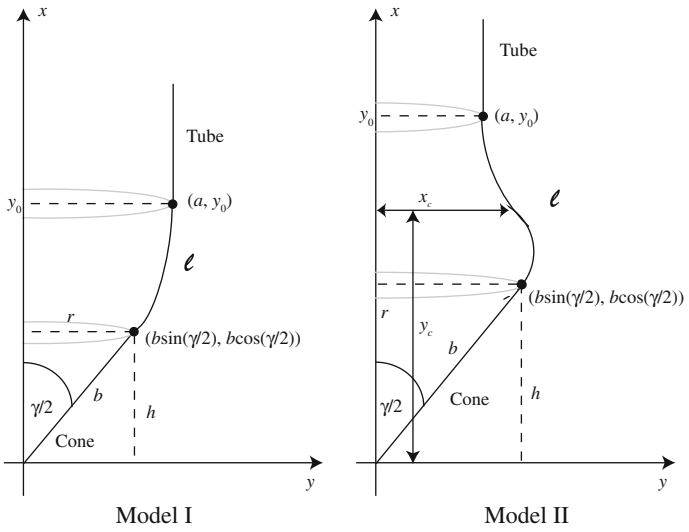

Fig. 1 Axially symmetric geometries for *Model I*, for which the join contains only positive curvature, and *Model II*, which has both positive and negative curvature in the join region

complicated discrete problem. Again, our major purpose is to attempt to capture the dominant features of the problem.

In the following section, we state the fundamental equations for the calculus of variations to model the joining region between the carbon nanocone and the carbon nanotube. In Sect. 3, the curvature is assumed to remain positive in the join region and we refer to this case as Model I. Model II is assumed to have two join regions, one of positive curvature and one of negative curvature and this model is presented in Sect. 4. Results and a discussion are given in Sect. 5 and a summary is presented in Sect. 6. Finally, "Appendix" contains the details for the analytical evaluation of the two asymptotic values μ_0 and μ_3 for the characteristic parameter defined by (13).

2 Continuous models

In this section we formulate the basic variational equations for a continuous approach to connect a carbon nanocone and a carbon nanotube. Specifically, the variational calculus is utilised to determine the curve adopted by a line smoothly connecting a cone base and a vertical carbon nanotube, such that the arc length of the join curve and the defect site at the cone base are specified. However, in terms of the rectangular Cartesian coordinates introduced below and shown in Fig. 1, the distance in the y-direction y_0 of the join to the cylindrical tube is not prescribed and it is determined as part of the solution. We comment that the same technique is successfully used in recent papers by the authors, Cox and Hill [8] and Baowan et al. [9] to determine the join regions between a carbon nanotube and a graphene sheet, and between two fullerenes, respectively.

Following the previous cited work of the authors, two distinct models are determined here which are illustrated in Fig. 1. For Model I, the join curvature is assumed to remain positive throughout the join, whereas for Model II two join regions are assumed, one of positive curvature and one of negative curvature. We position the nanocone of base radius r such that the cone vertex is assumed to be located at the origin of the (x, z)-plane as indicated in Fig. 1. A carbon nanotube of radius a is located with its axis co-linear with the y-axis starting from an unknown positive distance above the (x, z)-plane which we denote by y_0. Since the nanocone and the nanotube are rotationally symmetric about the y-axis, we can consider this as a problem in the two dimensional (x, y)-plane. The total prescribed arc length ℓ is assumed to connect a defect at $(r, h) = (b\sin(\gamma/2), b\cos(\gamma/2))$ and the tube at (a, y_0), where γ is the cone angle and $b = r\csc(\gamma/2)$ as shown in Fig. 1. We note that $(b\sin(\gamma/2), b\cos(\gamma/2))$ and (a, y_0) are the nearest atomic positions of the joined atoms on the cone base and on the tube open end, respectively, and there are five possibilities of the cone angle γ, which because of the assumption of axial symmetry we assume to be constant all around the cone vertex.

In the terminology of the calculus of variations, we wish to determine the function $y(x)$ which has an element of arc length ds, such that the function is an extremal of the following functional equation

$$J[y] = \int_0^{\ell} \kappa^2 ds + \lambda \int_0^{\ell} ds, \tag{1}$$

where κ is the curvature and λ is a Lagrange multiplier corresponding to the fixed length constraint. The arbitrariness of λ is used to determine the height of the join to the nanotube y_0 through (12) and (13) for Model I and (16) and (17) for Model II. We comment that in formulating the variational principle (1), there is some evidence that carbon nanotubes deform as in perfect elasticity, and rather like the elastica (see Zang et al. [10]). Further, in prescribing the fixed length constraint we have in mind that the join region will involve an integer number of bonds. For a two dimensional curve $y = y(x)$, we have $\kappa = y''/(1 + y'^2)^{3/2}$, $ds = (1 + y'^2)^{1/2}dx$, and the following equation may be deduced from (1)

$$J[y] = \int_a^{b\sin(\gamma/2)} \frac{y''^2}{(1 + y'^2)^{5/2}} dx + \lambda \int_a^{b\sin(\gamma/2)} (1 + y'^2)^{1/2} dx,$$

where primes throughout denote differentiation with respect to x. On applying the delta variational operator, we may derive the standard equation

$$\delta J[y] = \left[\left(F_{y'} - \frac{d}{dx} F_{y''} \right) \delta y + F_{y''} \delta y' \right]_a^{b\sin(\gamma/2)} + \int_a^{b\sin(\gamma/2)} \left(F_y - \frac{d}{dx} F_{y'} + \frac{d^2}{dx^2} F_{y''} \right) \delta y dx, \tag{2}$$

where subscripts denote partial derivatives and here F is given by

$$F(y', y'') = \frac{y''^2}{(1+y'^2)^{5/2}} + \lambda(1+y'^2)^{1/2}. \tag{3}$$

By imposing the continuity of the function y and its derivative, boundary conditions at the join to the nanocone are obtained, namely

$$y\left(b\sin\frac{\gamma}{2}\right) = b\cos\frac{\gamma}{2}, \qquad y'\left(b\sin\frac{\gamma}{2}\right) = \cot\frac{\gamma}{2}.$$

The height of the carbon nanotube, y_0 is unknown, so that for this endpoint we require the natural or alternative boundary condition which is derived from the first term in (2) and is given by

$$\left(F_{y'} - \frac{d}{dx}F_{y''}\right)\Big|_{x=a} = 0.$$

In Model I, the value of y' ranges from $\cot(\gamma/2)$ at $x = b\sin(\gamma/2)$ to ∞ at $x = a$, and therefore the boundary condition is $y'(a) = \infty$. In Model II, y' ranges from $\cot(\gamma/2)$ to ∞ where it changes sign and then ranges from $-\infty$ to some finite negative value before returning to $-\infty$. Therefore, in Model II, the boundary condition in $y'(a) = -\infty$.

The usual Euler–Lagrange equation is obtained from the second term in (2) which can be written as

$$F_y - \frac{d}{dx}F_{y'} + \frac{d^2}{dx^2}F_{y''} = 0.$$

Following Cox and Hill [8] on solving the above equation and invoking the above alternative boundary condition, we may deduce

$$F - y''F_{y''} = -\alpha, \tag{4}$$

where α is an arbitrary constant of integration, and from (3) into (4) we may obtain

$$\frac{y''^2}{(1+y'^2)^3} = \lambda + \frac{\alpha}{(1+y'^2)^{1/2}} = \kappa^2,$$

so that the curvature κ is given by

$$\kappa = \pm\left(\lambda + \frac{\alpha}{(1+y'^2)^{1/2}}\right)^{1/2}. \tag{5}$$

3 Model I: Positive curvature

From Fig. 1, the join curvature of Model I remains positive along the entire arc of length ℓ, so that only the positive case of (5) is considered. On making the substitution $y' = \tan\theta$, (5) becomes

$$\kappa = (\lambda + \alpha\cos\theta)^{1/2}, \tag{6}$$

and from the definition of curvature $\kappa = y''/(1 + y'^2)^{3/2}$, and making the same substitution for y', we may deduce

$$\frac{dy}{d\theta} = \frac{\sin\theta}{(\lambda + \alpha\cos\theta)^{1/2}}.$$

Following the previous work of the authors, we now introduce a new parametric variable ϕ to simplify this equation, which is defined by

$$\cos\theta = 1 - 2k^2\sin^2\phi, \tag{7}$$

where $k = [(\lambda + \alpha)/2\alpha]^{1/2}$, and we may deduce

$$\frac{dy}{d\phi} = 2\beta k\sin\phi,$$

where $\beta = (2/\alpha)^{1/2}$. Upon integrating both sides of the above equation and using the boundary condition at the point $(b\sin(\gamma/2), b\cos(\gamma/2))$ of attachment to the nanocone to determine the constant of the integration, we obtain

$$y(\phi) = 2\beta k(\cos\phi_0 - \cos\phi) + b\cos\frac{\gamma}{2}, \tag{8}$$

where $\phi_0 = \sin^{-1}\left(\left\{[1 - \sin(\gamma/2)]/2k^2\right\}^{1/2}\right)$ corresponds to $\theta = \pi/2 - \gamma/2$ at the point $(b\sin(\gamma/2), b\cos(\gamma/2))$. By using the boundary condition at the point (a, y_0) of the tube open end with $\phi_t = \sin^{-1}(1/\sqrt{2}k)$ where $\theta = \pi/2$, we may deduce

$$y_0 = 2\beta k(\cos\phi_0 - \cos\phi_t) + b\cos\frac{\gamma}{2}, \tag{9}$$

and we note that $\theta \in [\pi/2 - \gamma/2, \pi/2]$ for Model I.

By precisely the same method, the corresponding parametric equation for x is obtained, which is given by

$$\frac{dx}{d\theta} = \frac{\cos\theta}{(\lambda + \alpha\cos\theta)^{1/2}},$$

and after changing to the new parameter ϕ, we obtain

$$\frac{dx}{d\phi} = \beta \frac{(1 - 2k^2 \sin^2 \phi)}{(1 - k^2 \sin^2 \phi)^{1/2}} = \beta \left[2(1 - k^2 \sin^2 \phi)^{1/2} - \frac{1}{(1 - k^2 \sin^2 \phi)^{1/2}} \right].$$

Upon integration this yields

$$x(\phi) = b \sin \frac{\gamma}{2} + \beta\{2[E(\phi, k) - E(\phi_0, k)] - [F(\phi, k) - F(\phi_0, k)]\}, \quad (10)$$

where $F(\phi, k)$ and $E(\phi, k)$ denote the usual Legendre incomplete elliptic integrals of the first and second kinds, respectively, as defined by Byrd and Friedman [11]. By using the boundary condition at the point (a, y_0) on the open tube end, we have

$$a - b \sin \frac{\gamma}{2} = \beta\{2[E(\phi_t, k) - E(\phi_0, k)] - [F(\phi_t, k) - F(\phi_0, k)]\}. \quad (11)$$

From the arc length constraint, we obtain

$$\ell = \int_{b \sin(\gamma/2)}^{a} (1 + y'^2)^{1/2} dx.$$

On making the substitution $y' = \tan\theta$ and changing to the parameter ϕ defined by (7), we may deduce

$$\ell = \beta[F(\phi_t, k) - F(\phi_0, k)]. \quad (12)$$

By substituting (12) into (11), we may derive

$$\mu = 2 \left(\frac{E(\phi_t, k) - E(\phi_0, k)}{F(\phi_t, k) - F(\phi_0, k)} \right) - 1, \quad (13)$$

where $\mu = (a - b \sin(\gamma/2))/\ell$. Thus, for a prescribed a, b, γ and ℓ, (13) can be numerically solved to determine the value for k. By substituting k back into (12), the value of β can be determined and therefore y_0 can be obtained from (9).

4 Model II: Positive and negative curvatures

In this section, we proceed exactly as in Sect. 3 for the first region of positive curvature from the point of attachment at the nanocone $(b \sin(\gamma/2), b \cos(\gamma/2))$ up until the critical point (x_c, y_c) where the curvature changes sign. We then consider the second region from the critical point (x_c, y_c) to the point of attachment at the nanotube (a, y_0) throughout which the curvature is negative. The parameter value of θ as defined in

the previous subsection at the critical point is denoted by θ_c, and from geometrical considerations we find that $0 < \theta_c < \pi/2$.

The same procedure is applied to the region of positive curvature, and this region is bounded by the point where the curvature $\kappa = 0$, from (6) we may derive

$$\theta_c = \cos^{-1}\left(-\frac{\lambda}{\alpha}\right).$$

Employing the parameter variable ϕ as defined by (7), we have $\phi = \pi/2$ when $\theta = \theta_c$, and from (8) and (10), the parametric equations for y_c and x_c may be obtained as

$$y_c = 2\beta k \cos\phi_0 + b\cos\frac{\gamma}{2}, \tag{14}$$

$$x_c = b\sin\frac{\gamma}{2} + \beta\{2[E(k) - E(\phi_0, k)] - [K(k) - F(\phi_0, k)]\}, \tag{15}$$

where β, k and ϕ_0 are defined in Sect. 3, $F(\phi_0, k)$ and $E(\phi_0, k)$ are the usual incomplete elliptic integrals of the first and second kinds, respectively, and $K(k)$ and $E(k)$ are complete elliptic integrals of the first and second kinds, respectively.

In the second region, we take the negative sign in (5) and from similar considerations described in the previous section, we may deduce

$$\frac{dy}{d\phi} = -2\beta k \sin\phi.$$

By integrating both sides of the above equation, we derive

$$y(\phi) = 2\beta k(\cos\phi_0 + \cos\phi) + b\cos\frac{\gamma}{2},$$

where the constant of integration arises from the condition that $y = y_c$ when $\phi = \pi/2$ and then we use the expression (14) for y_c. From the boundary condition at the point of attachment to the carbon nanotube, we know that $\phi = \phi_t$ at the point (a, y_0), so that y_0 is given by

$$y_0 = 2\beta k(\cos\phi_0 + \cos\phi_t) + b\cos\frac{\gamma}{2}.$$

We note that the solution for y_0 in Model II differs only by a change in the sign of one term. Similarly, by taking the negative sign of (5) and solving for the parametric form of x with the expression (15) for x_c, we may deduce

$$x(\phi) = b\sin\frac{\gamma}{2} + \beta\{2[2E(k) - E(\phi, k) - E(\phi_0, k)] - [2K(k) - F(\phi, k) - F(\phi_0, k)]\}.$$

At the point (a, y_0) where $\phi = \phi_t$, we have

$$a - b\sin\frac{\gamma}{2} = \beta\{2[2E(k) - E(\phi_t, k) - E(\phi_0, k)] - [2K(k) - F(\phi_t, k) - F(\phi_0, k)]\}.$$

The arc length constraint is obtained from the two regions and we have

$$\ell = \int_{b\sin(\gamma/2)}^{x_c} (1 + y'^2)^{1/2} dx + \int_{x_c}^{a} (1 + y'^2)^{1/2} dx.$$

Again, by making the substitution $y' = \tan\theta$ and changing to the parameter ϕ, we may deduce

$$\ell = \beta[2K(k) - F(\phi_t, k) - F(\phi_0, k)]. \tag{16}$$

As before, the equation for $\mu = (a - b\sin(\gamma/2))/\ell$ is obtained by straightforward algebra and it can be written as

$$\mu = 2\left(\frac{2E(k) - E(\phi_t, k) - E(\phi_0, k)}{2K(k) - F(\phi_t, k) - F(\phi_0, k)}\right) - 1. \tag{17}$$

We observe that (17) only involves the single unknown k, and can be numerically solved for some prescribed μ to determine the value for k. By further substitution into (16), the value for β can be obtained and therefore, the attachment height y_0 can be calculated.

We observe that (13) of Model I coincides with (17) of Model II for the values $k = 1/\sqrt{2}$ and $k = \{[1 - \sin(\gamma/2)]/2\}^{1/2}$. When $k = 1/\sqrt{2}$, the value of μ is denoted by μ_1, and when $k = \{[1 - \sin(\gamma/2)]/2\}^{1/2}$, the value of μ is denoted by μ_2. A detailed numerical analysis of these equations is given in the following section.

5 Numerical results

Some general features of the solutions for Model I and Model II are examined in this section. Firstly, the solution, which is characterized by the nondimensional parameter $\mu = (a - b\sin(\gamma/2))/\ell$ subject to the constraint $-1 < \mu < 1$, is examined. In Fig. 2, we show the relation between the parameter μ and a new parameter $B = 1/k^2$, and this graph can be divided into two main regions. The first region is $\mu < \mu_0$ which corresponds to $B < 2$ and the second region is $\mu > \mu_0$ which corresponds to $B > 2/[1 - \sin(\gamma/2)]$ where μ_0 is the asymptotic value for μ as k tends to zero, which can be analytically determined, as presented in "Appendix", where it is shown to be

$$\mu_0 = 1 + \frac{\sqrt{2}(1 - \sqrt{2}\cos\omega)}{\ln[(\sqrt{2} - 1)/\tan(\omega/2)]},$$

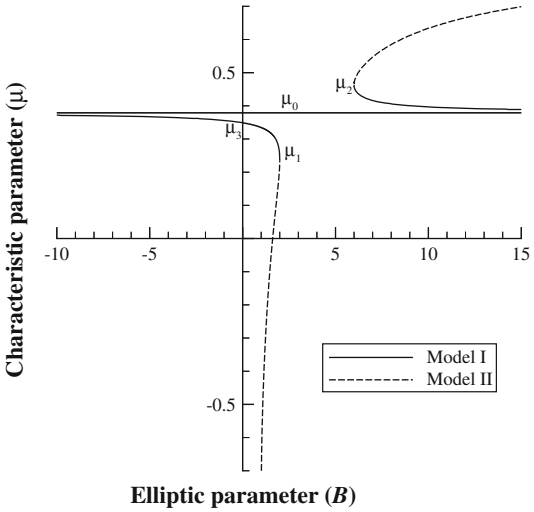

Fig. 2 Relation between the parameters $\mu = (a - b \sin(\gamma/2))/\ell$ and $B = 1/k^2$

where $\omega = (\pi - \gamma)/4$. We note that these two values of B arise when (13) and (17) coincide, as mentioned earlier.

The region of $\mu < \mu_0$ can be divided into three subregions, and the first subregion is $\mu_3 < \mu < \mu_0$ where μ_3 is the asymptotic value of μ as k tends to infinity. We find that the solution asymptotes with the line $\mu = \mu_0$, and crosses the vertical axis at the point μ_3 where μ_3 can be analytically determined, as shown in "Appendix", and it is found to be

$$\mu_3 = \frac{2}{\gamma}\left(1 - \cos\frac{\gamma}{2}\right).$$

In this case, the parameter B is negative, which corresponds to a negative value of α and an imaginary modulus k for the elliptic functions. The second subregion exists for $\mu_1 < \mu < \mu_3$ which corresponds to $0 < B \leq 2$, so that α is always positive and the modulus k is strictly real. The final subregion, which is obtained from Model II, applies for the range $-1 < \mu < \mu_1$ which corresponds to $1 < B \leq 2$, and again α is always positive.

The region of $\mu > \mu_0$ can be divided into two subregions, which are $\mu_0 < \mu < \mu_2$ from Model I and $\mu_2 < \mu < 1$ from Model II. The value of B is always positive in both of these subregions, and it corresponds to a negative value of α and a complex value of angle ϕ of the form $\phi = \pi/2 + i\varphi$. We note that in this region the curvature changes in sign from negative to positive. Furthermore, we note that the values μ given in (13) and (17) also depend on the cone angle γ, as depicted in Fig. 3 and the region for $\mu > \mu_0$ moves away from the origin as γ increases.

We now apply the solution of the continuous approach to a nondimensionalised situation which is shown in Figs. 4 and 5 for Model I and Model II, respectively. For purposes of comparison, the cone heights are assumed to be equal and the cone radii are obtained from $r = h \tan(\gamma/2)$. In addition, the fixed arc length is assumed to be

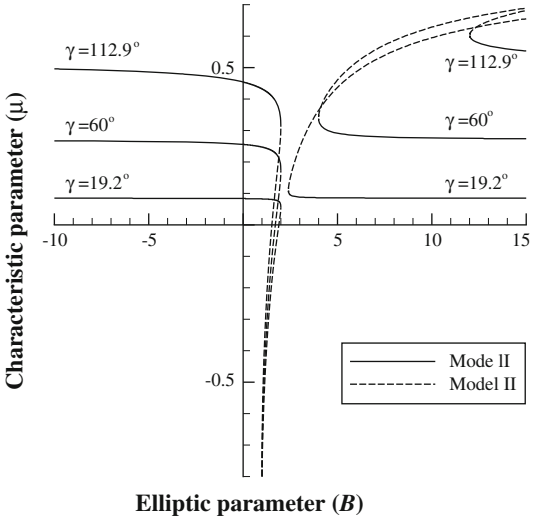

Fig. 3 Relation between the parameters μ and B for $\gamma = 112.9°, 60°$ and $19.2°$

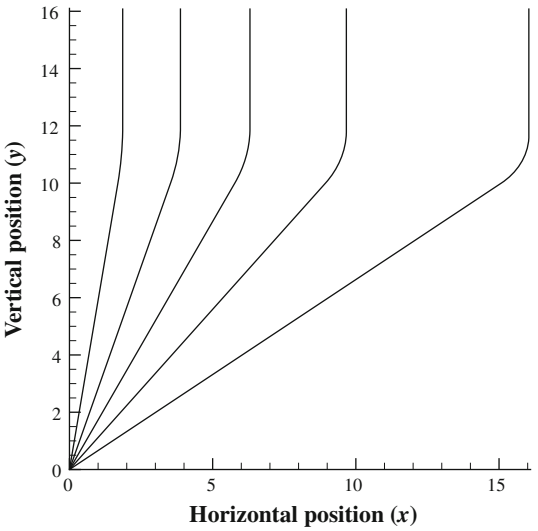

Fig. 4 Plots of joins $y = y(x)$ for Model I for five possible carbon nanocones, $\ell = 2$ and $B = -4.0$

$\ell = 2$ for all five possible carbon nanocones. We comment that a closer examination of the join regions shown in Figs. 4 and 5, show that they connect perfectly smoothly as shown in Fig. 6.

6 Summary

In this paper we use conventional applied mathematical modelling and the calculus of variations to determine a continuous approximation to the inherently discrete problem of finding the join connecting a carbon nanocone to a carbon nanotube. Such a

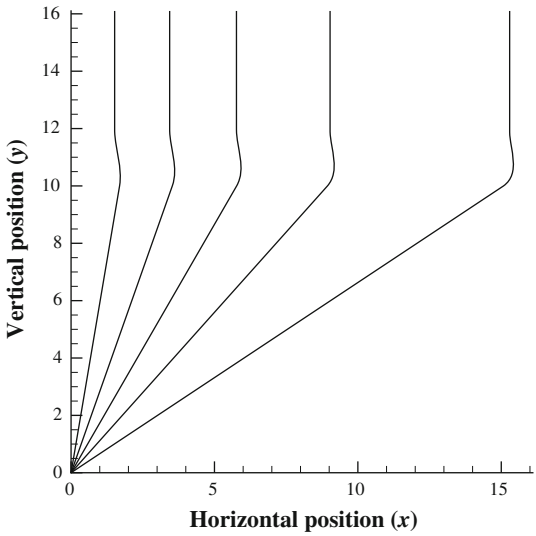

Fig. 5 Plots of joins $y = y(x)$ for Model II for five possible carbon nanocones, for $\ell = 2$ and $B = 1.7$

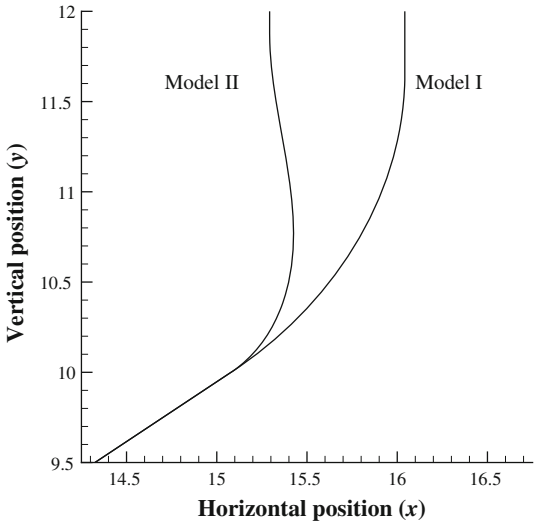

Fig. 6 Magnified plot of connection for $\gamma = 112.9°$ and for both Models I and II

combined nanostructure would have application as a probe for a scanning tunnelling microscope. All five possible carbon nanocones are considered each giving rise to a prescribed cone base radius and cone height. The calculus of variations is utilised to model the join and two distinct models are assumed which depend on the sign of the curvature. Furthermore, the system is assumed to be axially symmetric so that the problem may be reduced to two dimensions. In adopting this assumption, we recognise that real physical composite structures have undulations induced from the pentagons in the cone. These undulations are believed to be small, and the major purpose here is to formulate the underlying axially symmetric model, so that we have a reference

basis for the comparison of real physical structures. Although there are no experimental or computational results for comparison, these simple models appear to give rise to meaningful approximations to complex structures and therefore might be useful for future work on this problem.

Acknowledgments The support of the Australian Research Council, both through the Discovery Project Scheme and for providing an Australian Professorial Fellowship for JMH is gratefully acknowledged.

Appendix: Derivations for μ_0 and μ_3

Analytical derivations for the asymptotic values of μ_0 and μ_3 are presented in this appendix. These formulae are not immediately apparent from (13) and follow only after re-arrangement of (13) to the particular form (20) given below. Firstly, we consider the usual Legendre incomplete elliptic integral of the first kind $F(\phi, k)$, as defined by Byrd and Friedman [11], and for the value of ϕ when $\phi \in (\phi_t, \phi_0)$, we may deduce

$$F(\phi_t, k) - F(\phi_0, k) = \int_{\phi_0}^{\phi_t} \frac{d\phi}{\sqrt{1 - k^2 \sin^2 \phi}},$$

where $\phi_t = \sin^{-1}(1/\sqrt{2}k)$ and $\phi_0 = \sin^{-1}\left(\left\{[1 - \sin(\gamma/2)]/2k^2\right\}^{1/2}\right)$, and γ is the cone angle. On making the substitution $k \sin\phi = \sin\lambda$, we may derive

$$F(\phi_t, k) - F(\phi_0, k) = \int_{\pi/4-\gamma/4}^{\pi/4} \frac{d\lambda}{\sqrt{k^2 - \sin^2 \lambda}}. \tag{18}$$

By precisely the same considerations for the incomplete elliptic integral of the second kind $E(\phi, k)$ for $\phi \in (\phi_t, \phi_0)$, we obtain

$$E(\phi_t, k) - E(\phi_0, k) = \int_{\pi/4-\gamma/4}^{\pi/4} \frac{\cos^2 \lambda}{\sqrt{k^2 - \sin^2 \lambda}} d\lambda. \tag{19}$$

By substitution of (18) and (19) into (13), we may derive

$$\mu = \left(2 \int_{\pi/4-\gamma/4}^{\pi/4} \frac{\cos^2 \lambda \, d\lambda}{\sqrt{k^2 - \sin^2 \lambda}} - \int_{\pi/4-\gamma/4}^{\pi/4} \frac{d\lambda}{\sqrt{k^2 - \sin^2 \lambda}} \right) \times \left(\int_{\pi/4-\gamma/4}^{\pi/4} \frac{d\lambda}{\sqrt{k^2 - \sin^2 \lambda}} \right)^{-1}. \tag{20}$$

For μ_0, which is the asymptotic value as k tends to zero, by using $\cos 2\theta = 2\cos^2\theta - 1 = 1 - 2\sin^2\theta$, (20) can be formally reduced, and μ_0 becomes

$$\mu_0 = 1 - 2\int_{\omega}^{\pi/4} \sin\lambda\, d\lambda \left(\int_{\omega}^{\pi/4} \frac{d\lambda}{\sin\lambda}\right)^{-1},$$

where $\omega = (\pi - \gamma)/4$. On evaluating the above equation, we obtain

$$\mu_0 = 1 + \frac{\sqrt{2}(1 - \sqrt{2}\cos\omega)}{\ln[(\sqrt{2}-1)/\tan(\omega/2)]}.$$

For μ_3, which is the asymptotic value as k tends to infinity, we have from (20)

$$\mu_3 = \left(2\int_{\omega}^{\pi/4} \cos^2\lambda\, d\lambda - \int_{\omega}^{\pi/4} d\lambda\right)\left(\int_{\omega}^{\pi/4} d\lambda\right)^{-1},$$

and from which we may deduce

$$\mu_3 = \frac{2[1 - \cos(\gamma/2)]}{\gamma}.$$

References

1. K. Sattler, Carbon **33**, 915 (1995)
2. M. Ge, K. Sattler, Chem. Phys. Lett. **220**, 192 (1994)
3. A. Krishnan, E. Dujardin, M.M.J. Treacy, J. Hugdahl, S. Lynum, T.W. Ebbesen, Nature **388**, 451 (1997)
4. J.C. Charlier, G.M. Rignanese, Phys. Rev. Lett. **86**, 5970 (2001)
5. R. Pincak, V.A. Osipov, Phys. Lett. A **314**, 315 (2003)
6. C.M. Yeh, M.Y. Chen, J. Hwang, J.-Y. Gan, C.S. Kou, Nanotechnology **17**, 5930 (2006)
7. H. Zhang, P.X. Feng, V.I. Makarov, L. Fonseca, G. Morell, B.R. Weiner, J. Phys. D Appl. Phys. **42**, 035409 (2009)
8. B.J. Cox, J.M. Hill, J. Phys. A Math. Theor. **41**, 125203 (2008)
9. D. Baowan, B.J. Cox, J.M. Hill, Phil. Mag. **88**, 2953 (2008)
10. J. Zang, A. Treibergs, Y. Han, Liu Feng, Phys. Rev. Lett. **92**, 105501 (2004)
11. P.F. Byrd, M.D. Friedman, *Handbook of Elliptic Integrals for Engineers and Scientists*, 2nd edn. (Springer, Berlin, 1971)